Electronic Supplementary Material (ESI) for Physical Chemistry Chemical Physics.
This journal is © the Owner Societies 2022

# Supplementary information (SI) for Role of Magnetization on Catalytic Pathways of Non-Oxidative Methane Activation on Neutral Iron Carbide Clusters†

Manish Kumar,† Manzoor Ahmad Dar,†,‡ Ankita Katiyar,† Ravi Agrawal,¶ Prathamesh M. Shenai,¶ and Varadharajan Srinivasan*,†

†*Department of Chemistry, Indian Institute of Science Education and Research Bhopal, Bhopal 462 066, India*

‡*Department of Chemistry, Islamic University of Science and Technology, Awantipora, Jammu and Kashmir 192122, India*

¶*Shell India Markets Pvt. Ltd., Bangalore 562149, India*

E-mail: vardha@iiserb.ac.in

# 1 Choice of exchange-correlation functional

DFT functional - PBE,[1] BP86,[2,3] BPW91,[2,4] OPBE,[5] M06L,[6] B3LYP(*) (15% Hartree-Fock exact exchange),[7] and TPSSh[8] - and basis sets - 6-311++G(2d,2p),[9] def2TZVP,[10,11] def2QZVP,[10] S6-31G*,[12] and TZVP[13] - were considered.

First, we calculated the order of spin state energy of singlet, triplet, quintet, and septet for FeC diatomic cluster. We found that when the calculation is initiated with singlet state ($\hat{S}^2 = 0$), it ends up in a contaminated state for all functionals and basis sets (see Table S1). Hybrid and meta-GGA functionals (B3LYP(*), TPSSh, and M06L) give more spin contamination than the GGA functionals (Table S1). Except for B3LYP(*) and M06L, when calculations initiated with triplet spin state ($\hat{S}^2 = 2$), it ended up in state with $\hat{S}^2$ value within 10% error compared to the starting $\hat{S}^2$ (Table S2). Quintet and septet shows almost no contamination (Table S3 and S4). The order of spin states is similar in all the cases. The relative energies of the states vary. However, the triplet is the ground spin state for the FeC cluster.

To benchmark the DFT methods against the reaction mechanism, it is essential to examine the functionals and the basis sets for the bond dissociation energy (BDE) of FeC, $C_2$ and C-H bond in $CH_4$. The BDEs of FeC are shown in Table S5. All the functionals overestimated the BDE of FeC. The BDE of FeC is most accurately described by M06L followed by TPSSh for almost all the basis sets (Table S5). In combination with def2TZVP, M06L and TPSSh show the 1.19% and 2.08% error in BDE of FeC. It can be noticed that there is not much difference due to change in the basis set except for S6-31G*, which increases the error in BDE (Table S5). Therefore, we considered only the def2TZVP basis set for further calculations. We also calculated Fe-C bond length using def2TZVP and found that all functional give percentage error in bond length up to 2.34% (Table S6). In terms of Fe-C bond length, all functional perform well. Notably, B3LYP(*) give largest error in BDE (see Table S5).

BDE of $C_2$ and C-H are also calculated only for def2TZVP. Table S7 shows that, in C-H

BDE, the maximum error is given by BP86 (7.16%) and the least error by BPW91 (3.64%). PBE, OPBE, M06L, and TPSSh give errors of 4.85%, 5.43%, 6%, and 5.61%, respectively. All the functionals behave reasonably well for C-H BDE as well. However, TPSSh shows the smallest error for $C_2$ BDE (0.48%) whereas PBE, OPBE, and M06L show the error of 11.9%, 8.2%, and 6.05%, respectively (see Table S8). Since the considered iron carbide clusters involve Fe-C and C-C bonds, TPSSh is the best functional due to its very small percentage error in Fe-C and $C_2$ BDE. OPBE is a computationally cheaper functional suggested in the literature for accuracy of spin states, which also perform well except for the Fe-C BDE in the present context. As a reasonable compromise between computational expense and accuracy, we propose using OPBE to obtained equilibrium geometries and correcting their energy with TPSSh. Applying this approach to the calculation of FeC BDE we found that the percentage error decreases from 20.35% (OPBE) to 3% (TPSSh/OPBE) (Table S9). We further compared the methane activation mechanism on the FeC cluster (as shown in Figure 1 in the main text) calculated by optimizations using TPSSh and M06L (Table S11) with the one in which energy is calculated using TPSSh and M06L on the OPBE optimized structures (Table S11). It is found that the type of spin crossovers are maintained in all these cases. The key difference is that M06L shows a stronger adsorption energy (-0.20 eV) than both OPBE (0 eV) and TPSSh (-0.02 eV) (Table S11). Consequently, the C-H activation barrier is higher (0.81 eV) in the M06L case. However, the energy levels for the transition state in M06L and OPBE are nearly equal. On the other hand, when OPBE geometry is used to calculate the reaction path energy with M06L (i.e. M06L/OPBE) and TPSSh (i.e. TPSSH/OPBE), it is found that activation barriers are comparable in M06L/OPBE and TPSSh/OPBE. The adsorption energy in M06L becomes positive from negative, whereas that in the TPSSh case is similar to previously obtained by optimization by TPSSh. To calculate the adsorption energy, it is important to account for the dispersion correction. The adsorption energies of all the clusters presented in this chapter are corrected by dispersion correction. The relevant discussion is provided in the upcoming section. Interestingly, TPSSh and OPBE

yielded similar geometries (Table S11). Therefore, the reaction path energy calculated by TPSSh/OPBE is as good as the reaction path is calculated by TPSSh optimization. In this work, we have used OPBE for geometry optimization for all the further calculations, and then energies are corrected by TPSSh. To account for the weak interactions in adsorption of methane GD3BJ dispersion corrections further correct the adsorption energies.

We also tested these functionals on a trinuclear cluster ($Fe_3C$) to calculate the order of spin states starting from S = 0 to S = 9. Undectet (S = 5) state is found to be the ground state for $Fe_3C$ cluster. On ignoring the spin-contaminated solutions, nonet (S = 4) and septet (S = 3) are the first and second excited spin states, respectively. Exceptionally, M06L shows tridectet (S = 6) as a second excited state instead of septet inconsistent with the literature.[14] This further justifies the choice of TPSSh over M06L in this case.

**Table S1: Expectation value of total spin operator $\langle \hat{S}^2 \rangle$ obtained when calculation is initiated with singlet state for FeC cluster. The expected value of $\langle \hat{S}^2 \rangle$ is zero.**

| Functional | Basis set | | | | |
|---|---|---|---|---|---|
| | 6-311++G(2d,2p) | def2QZVP | def2TZVP | S6-31G* | TZVP |
| B3LYP(*) | 2.3 | 4.0 | 4.0 | 2.0 | 4.4 |
| PBE | 0.5 | 0.5 | 0.5 | 0.5 | 0.6 |
| BP86 | 0.5 | 0.5 | 0.5 | 0.4 | 0.5 |
| BPW91 | 0.6 | 0.5 | 0.5 | 0.5 | 0.6 |
| M06L | 3.0 | 2.7 | 2.6 | 2.6 | 3.0 |
| OPBE | 1.2 | 1.2 | 1.2 | 1.1 | 1.4 |
| TPSSh | 3.0 | 2.9 | 2.9 | 2.7 | 3.2 |

**Table S2: Percentage spin contamination obtained when calculation is initiated with triplet state for FeC cluster.**

| Functional | Basis set | | | | |
|---|---|---|---|---|---|
| | 6-311++G(2d,2p) | def2QZVP | def2TZVP | S6-31G* | TZVP |
| B3LYP(*) | 4.40 | 13.70 | 12.66 | 2.97 | 17.85 |
| PBE | 0.34 | 0.31 | 0.30 | 0.28 | 0.37 |
| BP86 | 0.28 | 0.26 | 0.25 | 0.23 | 0.31 |
| BPW91 | 0.43 | 0.39 | 0.37 | 0.33 | 0.46 |
| M06L | 6.51 | 9.69 | 7.87 | 7.14 | 16.44 |
| OPBE | 1.19 | 1.07 | 1.03 | 0.95 | 1.32 |
| TPSSh | 6.48 | 5.99 | 5.54 | 4.82 | 7.46 |

**Table S3: Percentage spin contamination obtained when calculation is initiated with quintet state for FeC cluster.**

| Functional | Basis set | | | | |
|---|---|---|---|---|---|
| | 6-311++G(2d,2p) | def2QZVP | def2TZVP | S6-31G* | TZVP |
| B3LYP(*) | 0.08 | 0.17 | 0.17 | 0.06 | 0.20 |
| PBE | 0.03 | 0.03 | 0.17 | 0.02 | 0.03 |
| BP86 | 0.02 | 0.03 | 0.03 | 0.02 | 0.03 |
| BPW91 | 0.03 | 0.04 | 0.02 | 0.03 | 0.04 |
| M06L | 0.27 | 0.26 | 0.03 | 0.18 | 0.20 |
| OPBE | 0.06 | 0.06 | 0.14 | 0.04 | 0.06 |
| TPSSh | 0.19 | 0.20 | 0.06 | 0.16 | 0.22 |

**Table S4: Percentage spin contamination obtained when calculation is initiated with septet state for FeC cluster.**

| Functional | Basis set | | | | |
|---|---|---|---|---|---|
| | 6-311++G(2d,2p) | def2QZVP | def2TZVP | S6-31G* | TZVP |
| B3LYP(*) | 0.0 | 0.0 | 0.0 | 0.0 | 0.0 |
| PBE | 0.0 | 0.0 | 0.0 | 0.0 | 0.0 |
| BP86 | 0.0 | 0.0 | 0.0 | 0.0 | 0.0 |
| BPW91 | 0.0 | 0.0 | 0.0 | 0.0 | 0.0 |
| M06L | 0.0 | 0.0 | 0.0 | 0.0 | 0.0 |
| OPBE | 0.0 | 0.0 | 0.0 | 0.0 | 0.0 |
| TPSSh | 0.0 | 0.0 | 0.0 | 0.0 | 0.0 |

**Table S5: Percentage error in bond dissociation energy (BDE) of FeC diatomic cluster. The reference energy of the BDE was adopted from ref.[15]**

| Functional | Basis set | | | | |
|---|---|---|---|---|---|
| | 6-311++G(2d,2p) | def2QZVP | def2TZVP | S6-31G* | TZVP |
| B3LYP(*) | 10.81 | 137.45 | 125.09 | 13.72 | 122.12 |
| BP86 | 28.25 | 29.23 | 28.87 | 30.90 | 28.27 |
| BPW91 | 24.25 | 25.23 | 24.85 | 26.93 | 24.94 |
| M06L | 1.12 | 0.57 | 1.19 | 3.46 | 0.41 |
| OPBE | 19.78 | 20.95 | 20.35 | 22.86 | 19.35 |
| PBE | 29.04 | 30.07 | 29.67 | 31.93 | 28.85 |
| TPSSh | 1.74 | 2.66 | 2.08 | 15.36 | 1.23 |

**Table S6: Percentage error in Fe-C bond length of FeC using variety of functionals with def2TZVP basis set. The reference bond length was adopted from ref.[16]**

| Functional | Bond length | |
|---|---|---|
| | Fe-C (Å) | % error |
| B3LYP(*) | 1.61 | 0.83 |
| BP86 | 1.56 | -2.33 |
| BPW91 | 1.56 | -2.20 |
| M06L | 1.60 | 0.60 |
| OPBE | 1.56 | -2.24 |
| PBE | 1.56 | -2.34 |
| TPSSh | 1.58 | -0.69 |
| Expt.[16] | 1.59 | - |

**Table S7: Percentage error in C-H bond dissociation energy (BDE) of methane using variety of functionals with def2TZVP basis set. The reference energy of the BDE was adopted from ref.[15]**

| Functional | BDE | % error |
|---|---|---|
| B3LYP(*) | 4.84 | 6.27 |
| BP86 | 4.88 | 7.16 |
| BPW91 | 4.72 | 3.64 |
| M06L | 4.82 | 6.00 |
| OPBE | 4.80 | 5.43 |
| PBE | 4.77 | 4.85 |
| TPSSh | 4.81 | 5.61 |
| Expt.[15] | 4.55 | - |

**Table S8: Percentage error in bond dissociation energy (BDE) of $C_2$ using variety of functionals with def2TZVP basis set. The reference energy of the BDE was adopted from ref.[15]**

| Functional | BDE | % error |
|---|---|---|
| B3LYP-star | 6.36 | 3.09 |
| BP86 | 6.80 | 10.27 |
| BPW91 | 6.69 | 8.40 |
| M06L | 6.54 | 6.05 |
| OPBE | 6.68 | 8.19 |
| PBE | 6.90 | 11.89 |
| TPSSh | 6.20 | 0.49 |
| expt.[15] | 6.17 | - |

**Table S9: Percentage error in Fe-C bond dissociation energy on the geometry optimized by OPBE using variety of functionals with def2TZVP basis set. The reference energy of the BDE was adopted from ref.[15]**

| Functional | BDE | % error |
|---|---|---|
| B3LYP(*) | 3.95 | 0.03 |
| BP86 | 5.15 | 30.37 |
| BPW91 | 4.99 | 26.35 |
| M06L | 4.03 | 1.92 |
| OPBE | 4.81 | 21.77 |
| PBE | 5.18 | 31.18 |
| TPSSh | 4.07 | 3.06 |
| Expt.[15] | 3.95 | - |

**Table S10: Methane binding energies calculated with TPSSh and TPSSh+GD2BJ.**

| Cluster | TPSSh + GD3BJ | TPSSh |
|---|---|---|
| FeC | -0.001 | 0.01 |
| $FeC_2$ | -0.41 | -0.33 |
| $FeC_3$ | -0.60 | -0.51 |
| $Fe_3C$ | -0.01 | -0.001 |
| $Fe_3C_3$ | -0.02 | -0.003 |
| $Fe_3C_6$ | -0.02 | -0.001 |
| $Fe_3C_9$ | -0.03 | -0.004 |
| $Fe_3C_6$−iso | -0.06 | -0.01 |
| $Fe_3C_9$−iso | -0.01 | 0.0001 |

**Table S11: The methane activation reaction mechanism on FeC cluster calculated using three different functionals. The complete reaction path is calculated geometry and transition state optimizations in all three functionals. The spin state of every structure presented have less 10% spin contamination. Bold numbers represent the lowest energy spin state for corresponding state. For explanation of energy term see main text.**

| State | OPBE | | | M06L | | | TPSSh | | |
|---|---|---|---|---|---|---|---|---|---|
| | Triplet | Quintet | Septet | Triplet | Quintet | Septet | Triplet | Quintet | Septet |
| IS | **0.00** | 0.87 | 2.16 | **0.00** | 0.76 | 1.64 | **0.00** | 0.88 | 1.76 |
| I1 | **0.00** | 0.85 | 2.15 | **-0.20** | 0.55 | 1.15 | **-0.02** | 0.84 | 1.43 |
| TS1 | **0.62** | 1.37 | 3.06 | **0.60** | 1.84 | 1.97 | **0.71** | 1.97 | 2.74 |
| I2 | -0.19 | **-0.38** | 0.42 | -0.61 | **-0.92** | -0.30 | -0.38 | **-0.62** | -0.23 |
| FS | **1.88** | 2.19 | 3.59 | **1.59** | 1.89 | 3.09 | **1.55** | 1.86 | 2.72 |
| $E_B$ | -0.003 | | | -0.205 | | | -0.016 | | |
| $E_{Act}$ | 0.621 | | | 0.808 | | | 0.731 | | |
| $E_{Evol}$ | | 2.571 | | | 2.808 | | | 2.480 | |
| $E_{Evol}^{eff}$ | | 2.263 | | | 2.515 | | | 2.173 | |
| $E_R$ | 1.880 | | | 1.595 | | | 1.555 | | |
| | | | | M06L/OPBE | | | TPSSh/OPBE | | |
| IS | **0.00** | 0.87 | 2.16 | **0.00** | 0.77 | 1.65 | **0.00** | 0.88 | 1.78 |
| I1 | **0.00** | 0.85 | 2.15 | **0.01** | 0.77 | 1.65 | **0.00** | 0.88 | 1.77 |
| TS1 | **0.62** | 1.37 | 3.06 | **0.63** | 1.25 | 2.60 | **0.72** | 1.43 | 2.75 |
| I2 | -0.19 | **-0.38** | 0.42 | -0.58 | **-0.84** | -0.28 | -0.37 | **-0.59** | -0.19 |
| FS | **1.88** | 2.19 | 3.59 | **1.61** | 1.91 | 3.12 | **1.56** | 1.88 | 2.78 |
| $E_B$ | -0.003 | | | 0.008 | | | -0.002 | | |
| $E_{Act}$ | 0.621 | | | 0.626 | | | 0.719 | | |
| $E_{Evol}$ | | 2.517 | | | 2.748 | | | 2.462 | |
| $E_{Evol}^{eff}$ | | 2.263 | | | 2.449 | | | 2.151 | |
| $E_R$ | 1.880 | | | 1.612 | | | 1.565 | | |

# 2 Spin contamination along the reaction path

**Table S12: Percentage spin contamination of all the structure along the reaction mechanism on mononucluear clusters.**

| Cluster | State | Multiplicities | | |
|---|---|---|---|---|
| $FeC_1$ | | Triplet | Quintet | Septet |
| | IS | 3.51 | .14 | 0 |
| | I1 | 3.50 | .14 | 0 |
| | TS1 | .31 | .04 | 0 |
| | I2 | .88 | .01 | 0 |
| | FS | .44 | 0 | 0 |
| $FeC_2$ | | Triplet | Quintet | Septet |
| | IS | 1.20 | 0 | 0 |
| | I1 | 1.33 | 0 | 0 |
| | TS1 | .12 | .01 | 0 |
| | I2 | .07 | 0 | 0 |
| | FS | .01 | 0 | 0 |
| $FeC_3$ | | Triplet | Quintet | Septet |
| | IS | .48 | .02 | .01 |
| | I1 | .61 | .01 | .01 |
| | TS1 | 2.46 | .02 | 0 |
| | I2 | 3.62 | .03 | 0 |
| | FS | .06 | 0 | 0 |

**Table S13: Percentage spin contamination of all the structure along the reaction mechanism on trinucluear clusters.**

| State | | Multiplicities | | |
|---|---|---|---|---|
| $Fe_3C$ | | Septet | Nonet | Undectet |
| | IS | 1.93 | .12 | .02 |
| | I1 | .88 | .12 | .02 |
| | I2 | 1.37 | .17 | .03 |
| | FS | .76 | .07 | .01 |
| $Fe_3C_3$ | | Septet | Nonet | Undectet |
| | IS | .24 | .10 | .05 |
| | I1 | .24 | .10 | .05 |
| | TS1 | .24 | .06 | .08 |
| | I2 | .48 | .14 | .04 |
| | FS | .22 | .11 | .02 |
| $Fe_3C_6$ | | Septet | Nonet | Undectet |
| | IS | 2.59 | .21 | 0 |
| | I1 | 1.47 | .21 | 0 |
| | TS1 | .84 | .04 | .02 |
| | I2 | 1.25 | .26 | .01 |
| | FS | 1.16 | .06 | 0 |
| $Fe_3C_9$ | | Septet | Nonet | Undectet |
| | IS | 1.06 | .44 | .02 |
| | I1 | 1.06 | .44 | .02 |
| | TS1 | .92 | .05 | .01 |
| | I2 | 1.06 | .05 | .01 |
| | FS | .59 | .02 | .01 |

**Table S14: Percentage spin contamination of all the structure along the reaction mechanism on high energy isomers of $Fe_3C_9$ and $Fe_3C_6$ trinucluear clusters.**

| | State | Multiplicities | | |
|---|---|---|---|---|
| $Fe_3C_6$−iso | | Nonet | Undectet | Tridectet |
| | IS | .09 | .02 | 0 |
| | I1 | .08 | .02 | 0 |
| | TS1 | .08 | .01 | 0 |
| | I2 | .10 | .03 | 0 |
| | FS | .06 | .01 | 0 |
| | | | | |
| $Fe_3C_9$−iso | | Septet | Nonet | Undectet |
| | IS | 3.12 | .59 | .21 |
| | I1 | 4.40 | .59 | .21 |
| | TS1 | 1.25 | .68 | .18 |
| | I2 | 1.04 | .36 | .14 |
| | FS | 1.10 | .26 | .07 |

# 3 Mulliken spin densities

**Table S15: Mulliken spin densities of all the structure along the reaction mechanism on all clusters.**

| | State | Fe | C | H | Unpaired electrons |
|---|---|---|---|---|---|
| **FeC** | | | | | |
| Triplet | | | | | |
| | IS | 2.91 | -0.91 | | 2.00 |
| | I1 | 2.91 | -0.91 | 0.00 | 2.00 |
| | TS1 | 2.12 | -0.07 | -0.05 | 2.00 |
| | I2 | 2.59 | -0.67 | 0.08 | 2.00 |
| | FS | 3.43 | -0.48 | 0.05 | 3.00 |
| Quintet | | | | | |
| | IS | 3.91 | 0.09 | | 4.00 |
| | I1 | 3.91 | 0.08 | 0.01 | 4.00 |
| | TS1 | 3.58 | 0.40 | 0.02 | 4.00 |
| | I2 | 3.39 | 0.57 | 0.04 | 4.00 |
| | FS | 3.84 | 1.17 | -0.01 | 5.00 |
| Septet | | | | | |
| | IS | 3.82 | 2.18 | | 6.00 |
| | I1 | 3.81 | 2.18 | 0.00 | 6.00 |
| | TS1 | 3.71 | 2.34 | -0.05 | 6.00 |
| | I2 | 4.11 | 1.89 | 0.00 | 6.00 |
| | FS | 5.05 | 1.96 | -0.01 | 7.00 |

| | State | Fe | C | H | Unpaired electrons |
|---|---|---|---|---|---|
| **$FeC_2$** | | | | | |
| Triplet | | | | | |
| | IS | 2.54 | -0.54 | | 2.00 |
| | I1 | 2.55 | -0.54 | 0.00 | 2.00 |
| | TS1 | 1.99 | 0.06 | -0.05 | 2.00 |
| | I2 | 2.13 | -0.14 | 0.02 | 2.00 |
| | FS | 2.94 | 0.07 | -0.01 | 3.00 |
| Quintet | | | | | |
| | IS | 3.38 | 0.62 | | 4.00 |
| | I1 | 3.31 | 0.68 | 0.01 | 4.00 |
| | TS1 | 3.23 | 0.85 | -0.07 | 4.00 |
| | I2 | 4.07 | -0.09 | 0.02 | 4.00 |
| | FS | 4.96 | 0.04 | -0.01 | 5.00 |
| Septet | | | | | |
| | IS | 4.92 | 1.08 | | 6.00 |
| | I1 | 4.92 | 1.08 | 0.00 | 6.00 |
| | TS1 | 4.21 | 1.43 | 0.35 | 6.00 |
| | I2 | 4.16 | 1.60 | 0.24 | 6.00 |
| | FS | 5.21 | 1.73 | 0.06 | 7.00 |
| **$FeC_3$** | | | | | |
| Triplet | | | | | |
| | IS | 2.26 | -0.26 | | 2.00 |
| | I1 | 2.29 | -0.28 | -0.01 | 2.00 |
| | TS1 | 2.60 | -0.61 | 0.01 | 2.00 |
| | I2 | 2.75 | -0.77 | 0.02 | 2.00 |
| | FS | 2.78 | 0.21 | 0.01 | 3.00 |
| Quintet | | | | | |
| | IS | 3.73 | 0.27 | | 4.00 |
| | I1 | 2.88 | 1.11 | 0.01 | 4.00 |
| | TS1 | 2.94 | 1.08 | -0.02 | 4.00 |
| | I2 | 3.35 | 0.62 | 0.03 | 4.00 |
| | FS | 3.51 | 1.50 | -0.01 | 5.00 |
| Septet | | | | | |
| | IS | 3.85 | 2.15 | | 6.00 |
| | I1 | 3.64 | 2.37 | -0.01 | 6.00 |
| | TS1 | 3.91 | 2.11 | -0.03 | 6.00 |
| | I2 | 4.09 | 1.93 | -0.02 | 6.00 |
| | FS | 5.09 | 1.96 | -0.05 | 7.00 |

| | State | Fe | C | H | Unpaired electrons |
|---|---|---|---|---|---|
| **$Fe_3C$** | | | | | |
| Septet | | | | | |
| | IS | 6.46 | -0.46 | | 6.00 |
| | I1 | 6.54 | -0.49 | -0.05 | 6.00 |
| | TS1 | 6.86 | -0.78 | -0.08 | 6.00 |
| | I2 | 6.47 | -0.48 | 0.01 | 6.00 |
| | FS | 7.37 | -0.38 | 0.00 | 7.00 |
| Nonet | | | | | |
| | IS | 8.81 | -0.81 | | 8.00 |
| | I1 | 8.82 | -0.80 | -0.02 | 8.00 |
| | TS1 | 8.74 | -0.68 | -0.06 | 8.00 |
| | I2 | 8.53 | -0.54 | 0.02 | 8.00 |
| | FS | 9.26 | -0.25 | -0.01 | 9.00 |
| Undectet | | | | | |
| | IS | 10.42 | -0.42 | | 10.00 |
| | I1 | 10.41 | -0.42 | 0.00 | 10.00 |
| | TS1 | 10.17 | -0.14 | -0.03 | 10.00 |
| | I2 | 10.26 | -0.29 | 0.03 | 10.00 |
| | FS | 11.13 | -0.17 | 0.04 | 11.00 |
| **$Fe_3C_3$** | | | | | |
| Septet | | | | | |
| | IS | 6.54 | -0.54 | | 6.00 |
| | I1 | 6.54 | -0.54 | 0.00 | 6.00 |
| | TS1 | 6.71 | -0.70 | -0.01 | 6.00 |
| | I2 | 7.14 | -1.17 | 0.03 | 6.00 |
| | FS | 7.74 | -0.74 | 0.00 | 7.00 |
| Nonet | | | | | |
| | IS | 8.12 | -0.12 | | 8.00 |
| | I1 | 8.12 | -0.13 | 0.00 | 8.00 |
| | TS1 | 8.07 | -0.07 | 0.00 | 8.00 |
| | I2 | 8.59 | -0.62 | 0.04 | 8.00 |
| | FS | 9.44 | -0.44 | 0.00 | 9.00 |
| Undectet | | | | | |
| | IS | 9.93 | 0.07 | | 10.00 |
| | I1 | 9.93 | 0.07 | 0.00 | 10.00 |
| | TS1 | 9.98 | 0.02 | 0.00 | 10.00 |
| | I2 | 9.96 | -0.01 | 0.05 | 10.00 |
| | FS | 10.46 | 0.52 | 0.02 | 11.00 |

| | State | Fe | C | H | Unpaired electrons |
|---|---|---|---|---|---|
| **$Fe_3C_6$** | | | | | |
| Septet | | | | | |
| | IS | 7.55 | -1.55 | | 6.00 |
| | I1 | 7.41 | -1.40 | -0.01 | 6.00 |
| | TS1 | 7.37 | -1.30 | -0.07 | 6.00 |
| | I2 | 7.24 | -1.26 | 0.02 | 6.00 |
| | FS | 8.12 | -1.14 | 0.01 | 7.00 |
| Nonet | | | | | |
| | IS | 8.69 | -0.69 | | 8.00 |
| | I1 | 8.69 | -0.69 | 0.00 | 8.00 |
| | TS1 | 8.12 | -0.05 | -0.07 | 8.00 |
| | I2 | 8.82 | -0.87 | 0.05 | 8.00 |
| | FS | 9.27 | -0.26 | -0.01 | 9.00 |
| Undectet | | | | | |
| | IS | 9.44 | 0.56 | | 10.00 |
| | I1 | 9.44 | 0.56 | 0.00 | 10.00 |
| | TS1 | 9.33 | 0.70 | -0.03 | 10.00 |
| | I2 | 9.62 | 0.35 | 0.03 | 10.00 |
| | FS | 9.92 | 1.08 | 0.00 | 11.00 |
| **$Fe_3C_9$** | | | | | |
| Septet | | | | | |
| | IS | 7.14 | -1.14 | | 6.00 |
| | I1 | 7.15 | -1.15 | 0.00 | 6.00 |
| | TS1 | 7.06 | -1.07 | 0.01 | 6.00 |
| | I2 | 7.25 | -1.29 | 0.04 | 6.00 |
| | FS | 8.15 | -1.16 | 0.00 | 7.00 |
| Nonet | | | | | |
| | IS | 9.12 | -1.12 | | 8.00 |
| | I1 | 9.13 | -1.13 | 0.00 | 8.00 |
| | TS1 | 8.25 | -0.26 | 0.01 | 8.00 |
| | I2 | 8.08 | -0.10 | 0.02 | 8.00 |
| | FS | 8.76 | 0.26 | -0.01 | 9.00 |
| Undectet | | | | | |
| | IS | 9.41 | 0.59 | | 10.00 |
| | I1 | 9.41 | 0.59 | 0.00 | 10.00 |
| | TS1 | 9.27 | 0.72 | 0.01 | 10.00 |
| | I2 | 9.35 | 0.60 | 0.05 | 10.00 |
| | FS | 9.98 | 1.00 | 0.02 | 11.00 |

| | State | Fe | C | H | Unpaired electrons |
|---|---|---|---|---|---|
| **$Fe_3C_6$−iso** | | | | | |
| Nonet | | | | | |
| | IS | 8.05 | -0.05 | | 8.00 |
| | I1 | 8.05 | -0.06 | 0.00 | 8.00 |
| | TS1 | 8.06 | -0.08 | 0.02 | 8.00 |
| | I2 | 8.33 | -0.35 | 0.02 | 8.00 |
| | FS | 9.13 | -0.12 | -0.01 | 9.00 |
| Undectet | | | | | |
| | IS | 9.57 | 0.43 | | 10.00 |
| | I1 | 9.57 | 0.42 | 0.00 | 10.00 |
| | TS1 | 9.42 | 0.57 | 0.01 | 10.00 |
| | I2 | 9.65 | 0.32 | 0.02 | 10.00 |
| | FS | 10.37 | 0.65 | -0.02 | 11.00 |
| Tridectet | | | | | |
| | IS | 10.87 | 1.13 | | 12.00 |
| | I1 | 10.87 | 1.13 | 0.00 | 12.00 |
| | TS1 | 10.81 | 1.19 | 0.00 | 12.00 |
| | I2 | 10.81 | 1.17 | 0.02 | 12.00 |
| | FS | 11.49 | 1.48 | 0.03 | 13.00 |
| **$Fe_3C_9$−iso** | | | | | |
| Septet | | | | | |
| | IS | 8.00 | -2.00 | | 6.00 |
| | I1 | 8.23 | -2.23 | 0.00 | 6.00 |
| | TS1 | 7.44 | -1.44 | 0.00 | 6.00 |
| | I2 | 7.24 | -1.27 | 0.03 | 6.00 |
| | FS | 8.47 | -1.47 | 0.00 | 7.00 |
| Nonet | | | | | |
| | IS | 8.98 | -0.98 | | 8.00 |
| | I1 | 8.99 | -0.99 | 0.00 | 8.00 |
| | TS1 | 8.90 | -0.94 | 0.04 | 8.00 |
| | I2 | 8.36 | -0.35 | -0.01 | 8.00 |
| | FS | 9.04 | -0.02 | -0.02 | 9.00 |
| Undectet | | | | | |
| | IS | 9.52 | 0.48 | | 10.00 |
| | I1 | 9.53 | 0.47 | 0.00 | 10.00 |
| | TS1 | 9.52 | 0.46 | 0.02 | 10.00 |
| | I2 | 9.37 | 0.61 | 0.02 | 10.00 |
| | FS | 9.65 | 1.37 | -0.02 | 11.00 |

# 4 Geometries of intermediates and transition states in all spin channels

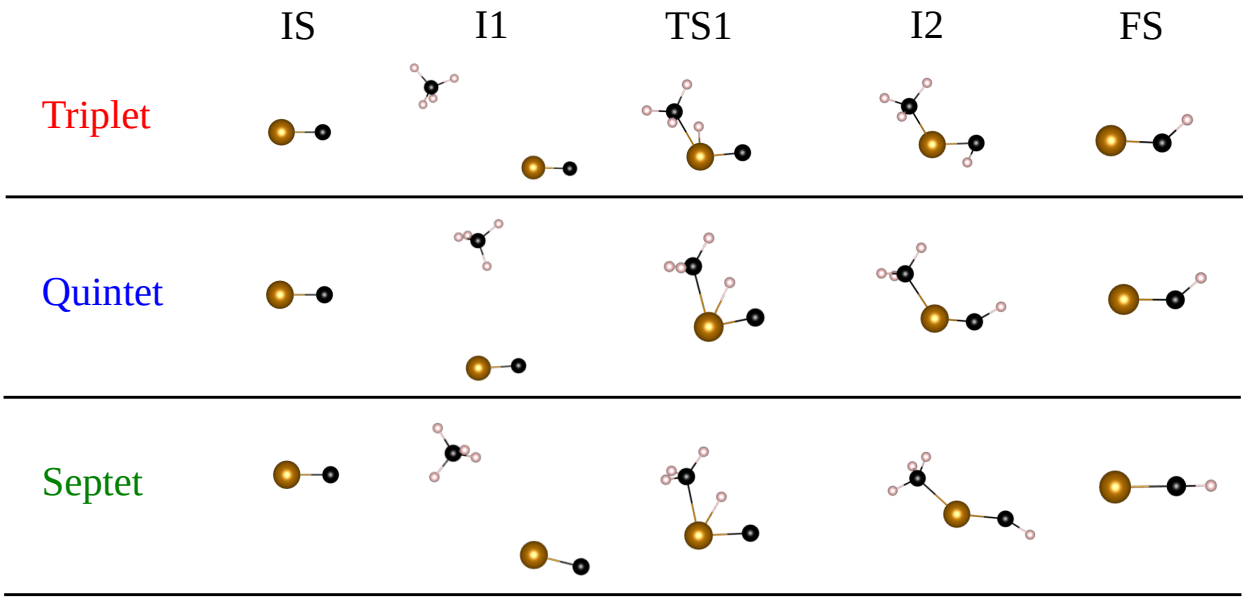


(a) FeC

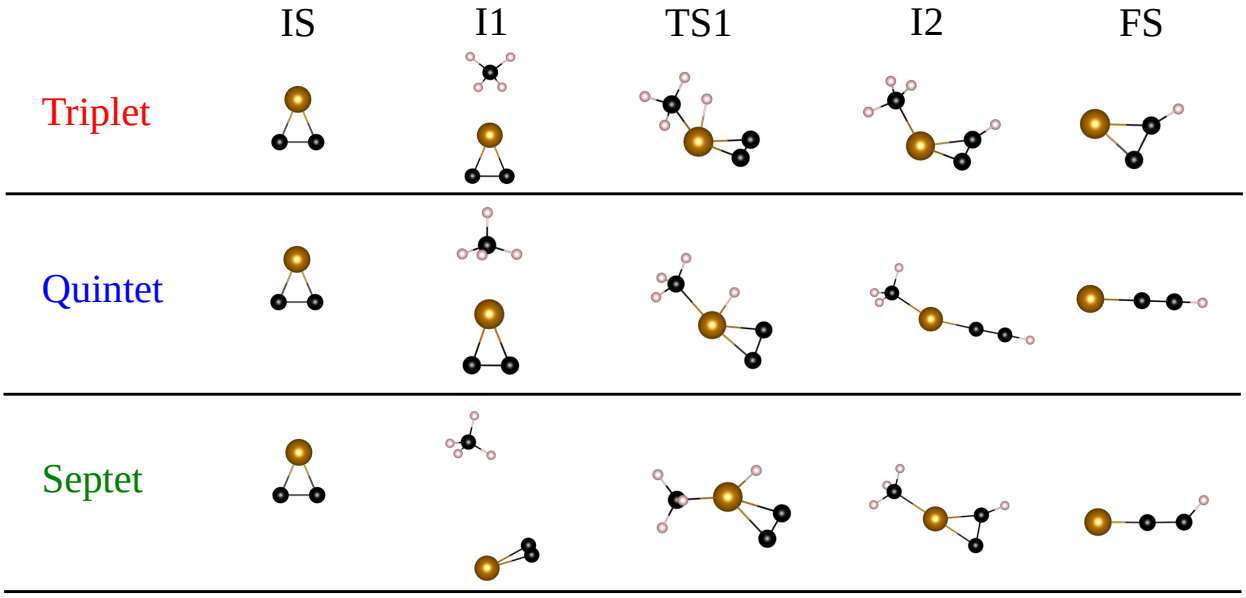


(b) $FeC_2$

Figure S1: Continued to next page...

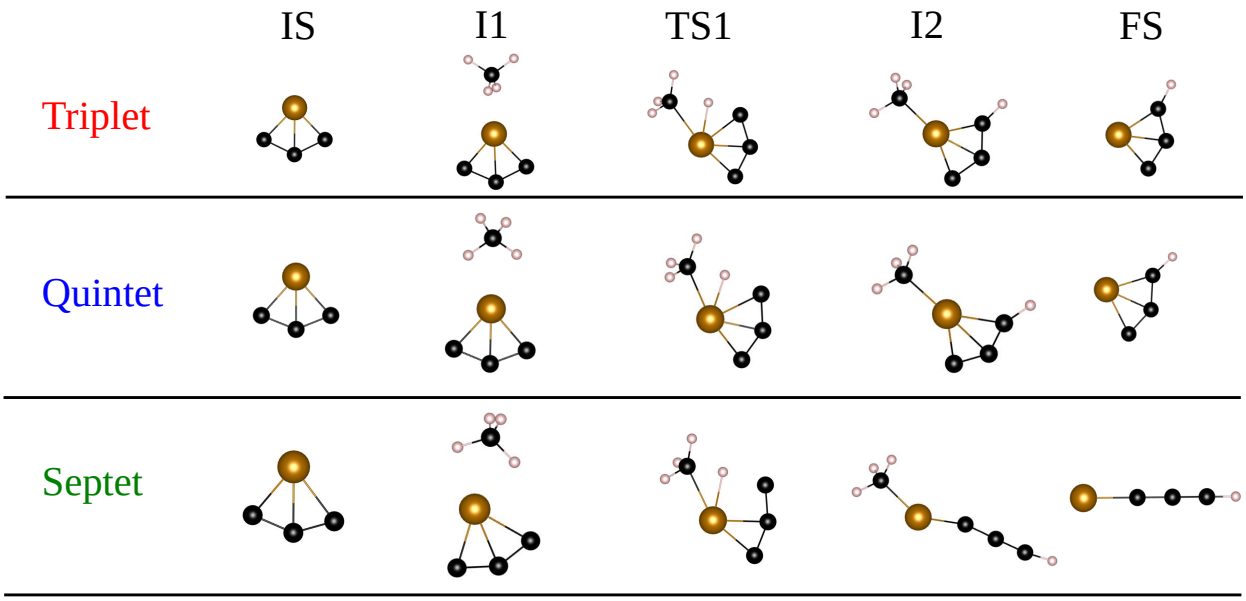


(c) $FeC_3$

Figure S1: Geometries of all the intermediates and transition states in all three spin channels studied for the reaction on mononuclear clusters. The spin multiplicity of the FS state is one unit higher in all spin channels (i.e., quartet in triplet channel, sextet in quintet channel, etc.) due to the evolution of the methyl radical.

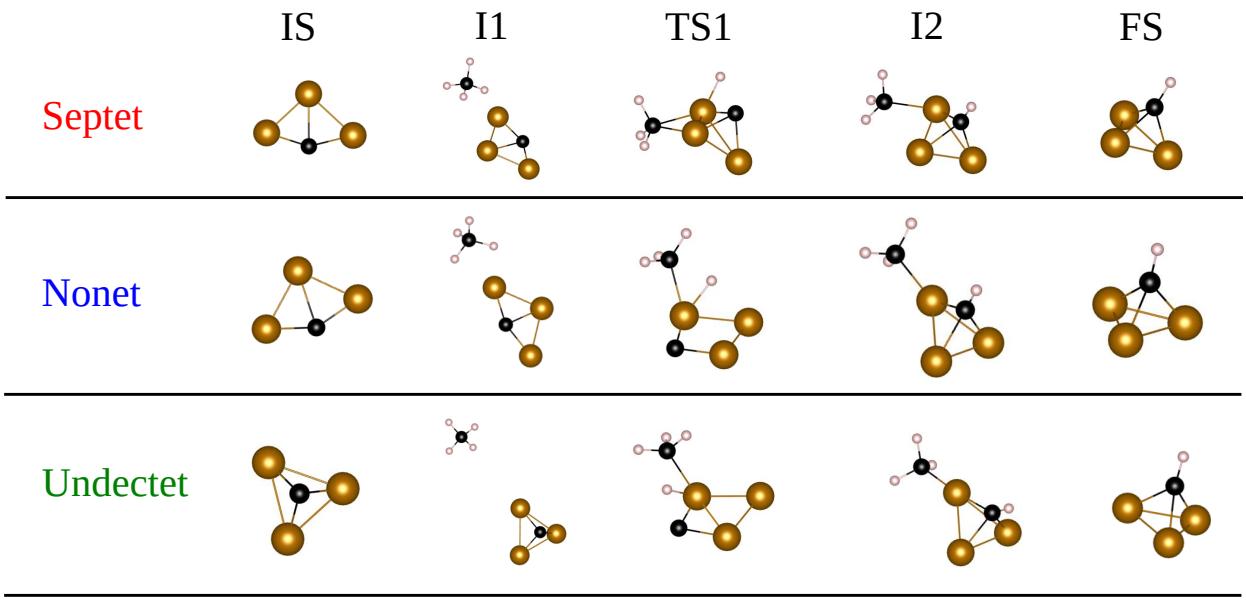


(a) $Fe_3C$

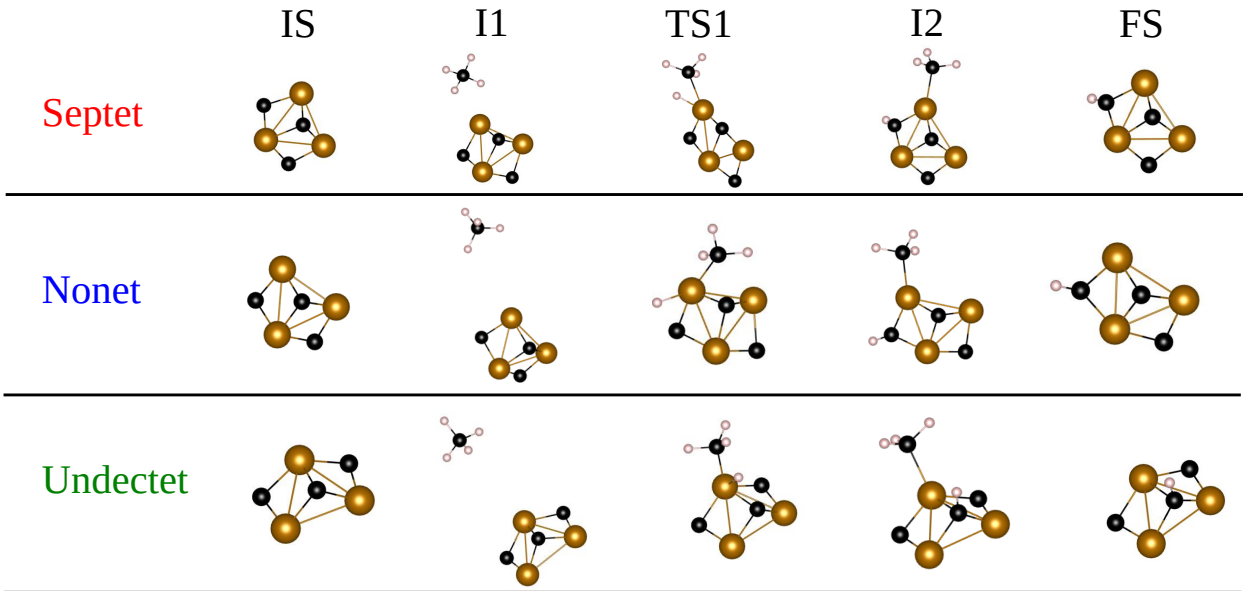


(b) $Fe_3C_3$

Figure S2: Continued to next page...

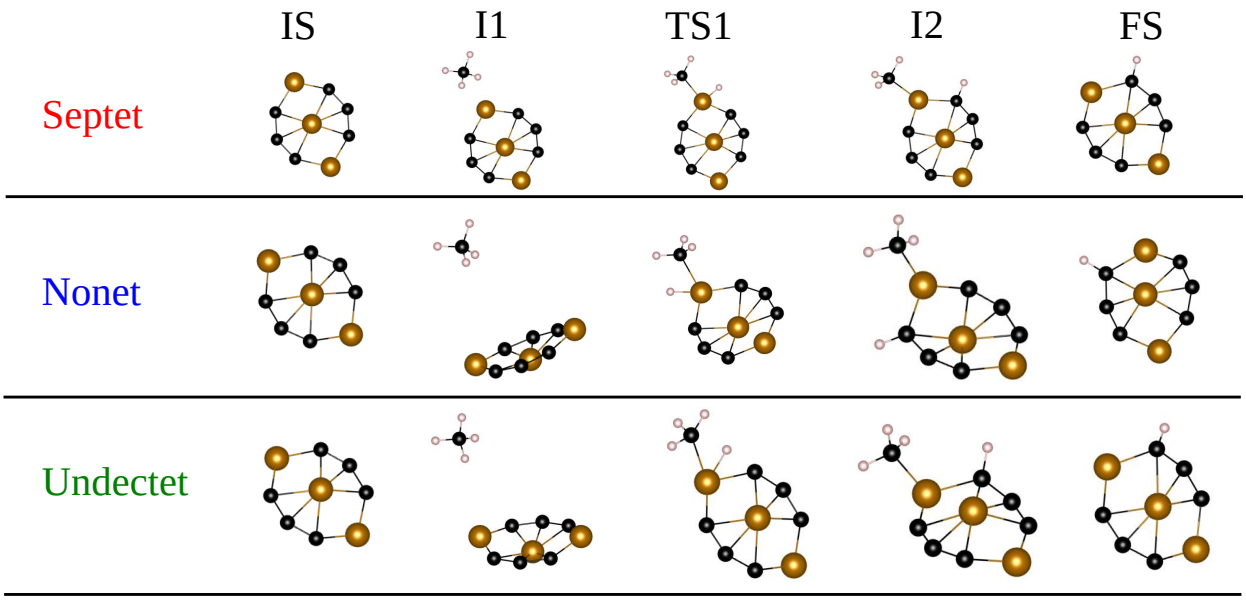


(c) $Fe_3C_6$

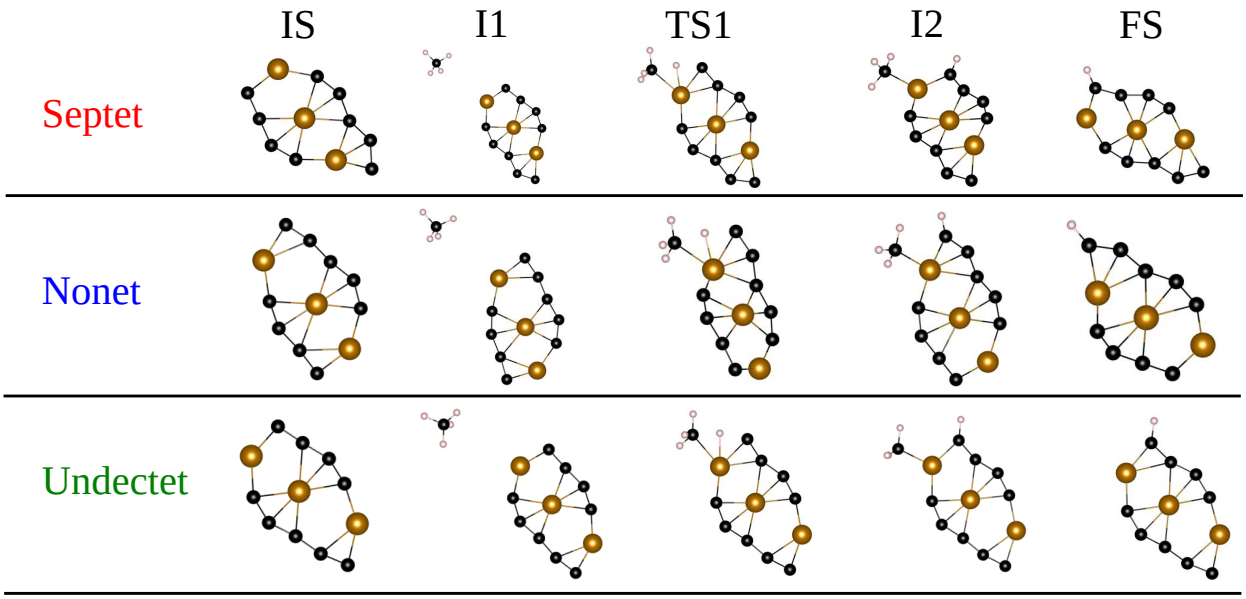


(d) $Fe_3C_9$

Figure S2: Geometries of all the intermediates and transition states in all three spin channels studied for the reaction on trinuclear clusters. The spin multiplicity of the FS state is one unit higher in all spin channels (i.e., octet in septet channel, dectet in nonet channel, etc.) due to the evolution of the methyl radical.

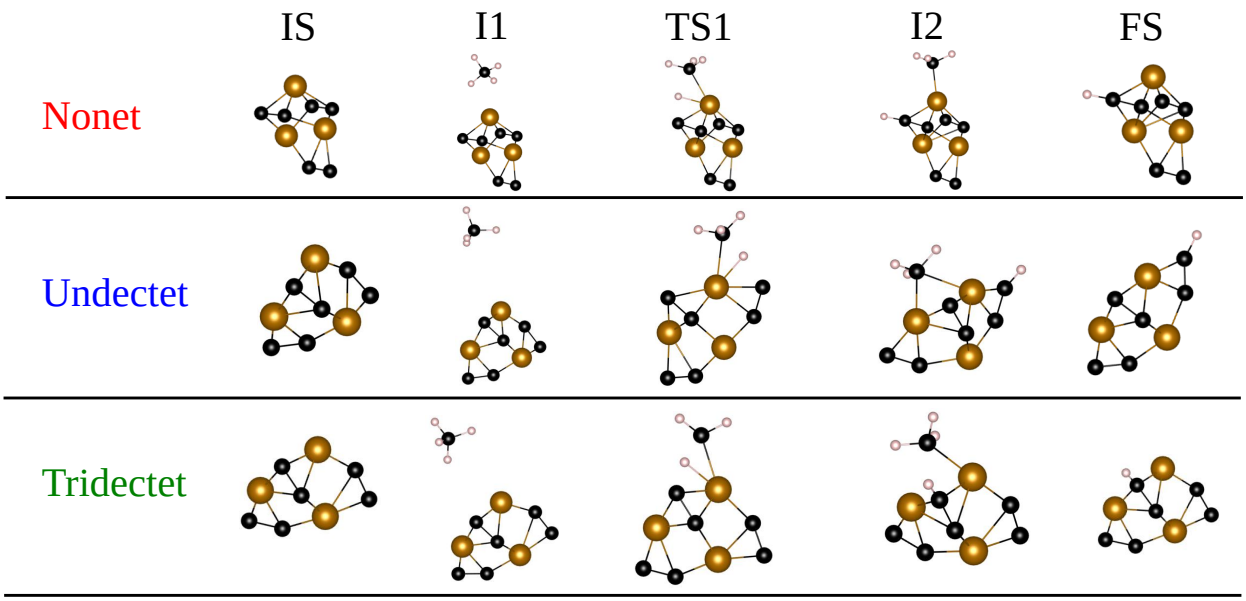


(a) $Fe_3C_6$−iso

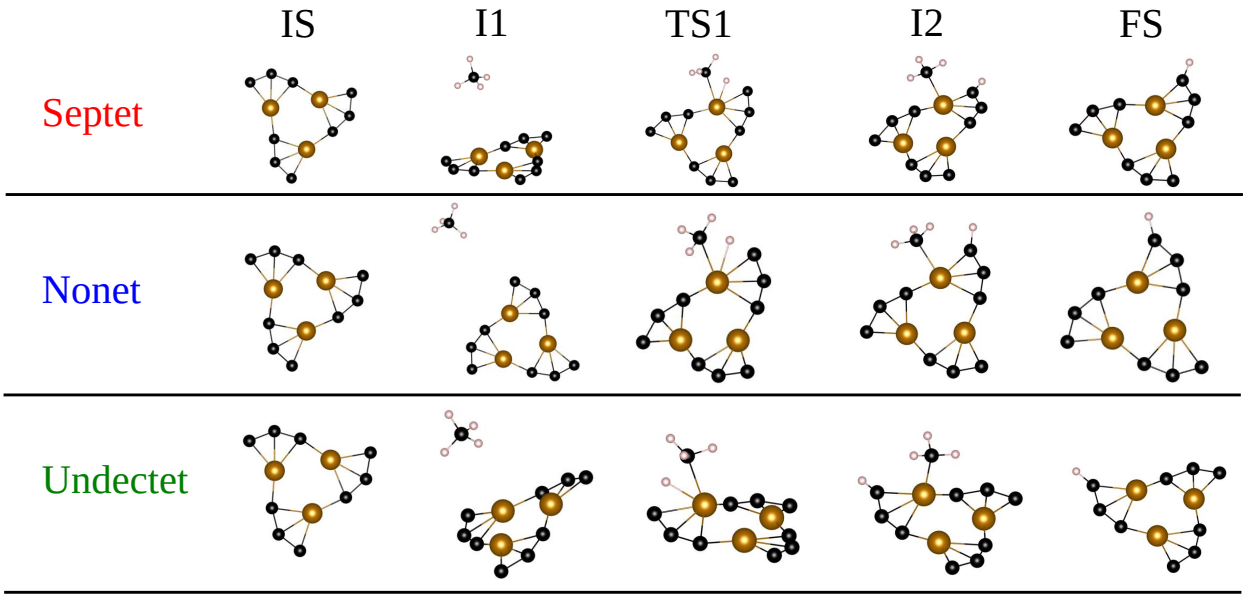


(b) $Fe_3C_9$−iso

Figure S3: Geometries of all the intermediates and transition states in all three spin channels studied for the reaction on high energy isomers of $Fe_3C_6$−iso and $Fe_3C_9$−iso clusters. The spin multiplicity of the FS state is one unit higher in all spin channels (i.e., octet in septet channel, dectet in nonet channel, etc.) due to the evolution of the methyl radical.

# 5 Orbital diagrams

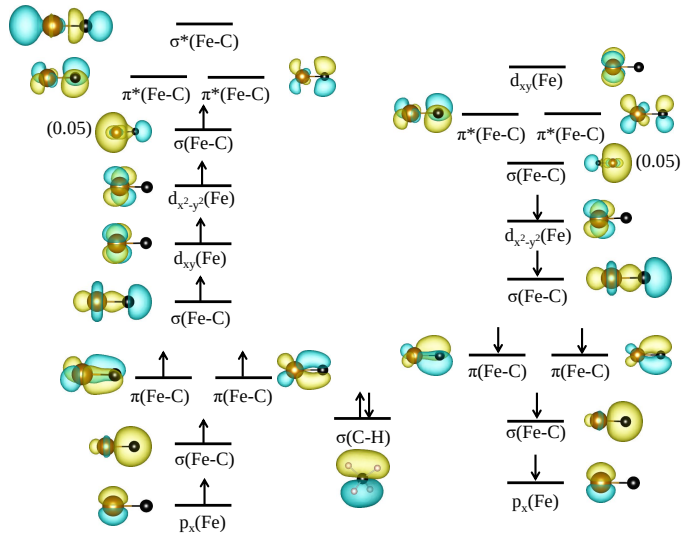


(a) IS

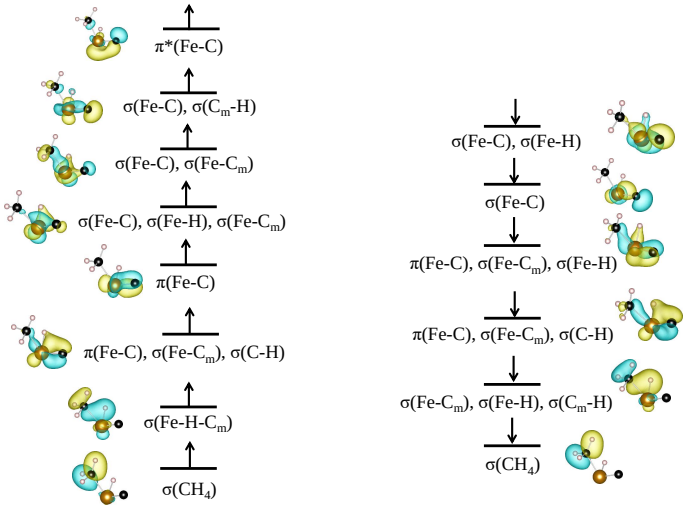


(b) TS1

Figure S4: Kohn-Sham orbital diagram of methane activation process on diatomic FeC cluster for IS and TS1. The up and down arrows represent the alpha and beta spin electrons. The isosurface value used is 0.07 $a_0^{-3}$ except alpha-HOMO and beta-LUMO in (a) where the isosurface value of 0.05 $a_0^{-3}$ as specified in parenthesis near the corresponding orbitals.

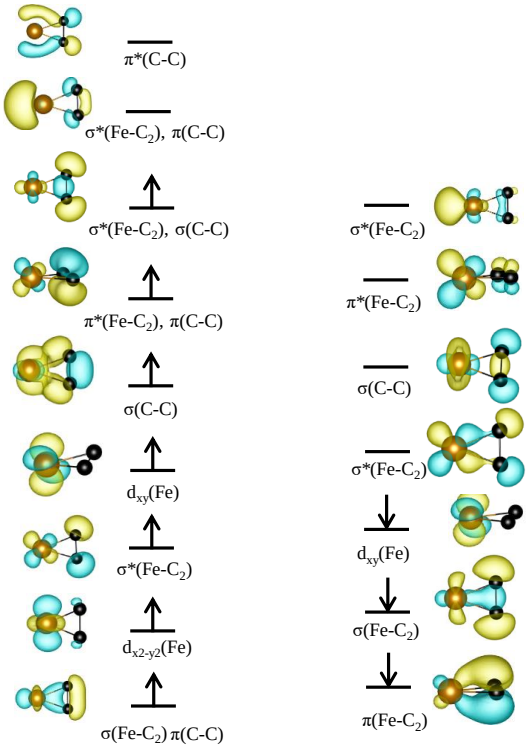


(a) IS

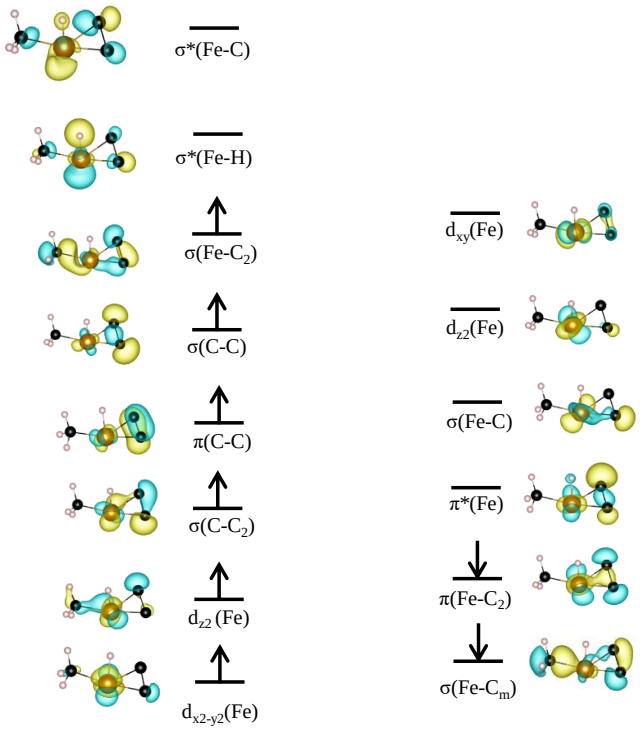


(b) TS1

Figure S5: Kohn-Sham orbital diagram of methane activation process on triatomic $FeC_2$ cluster for IS and TS1. The up and down arrows represent the alpha and beta spin electrons. The isosurface value used is 0.07 $a_0^{-3}$.

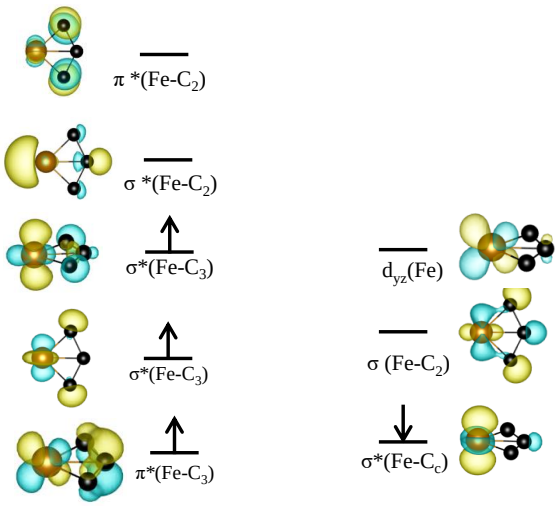


(a) IS

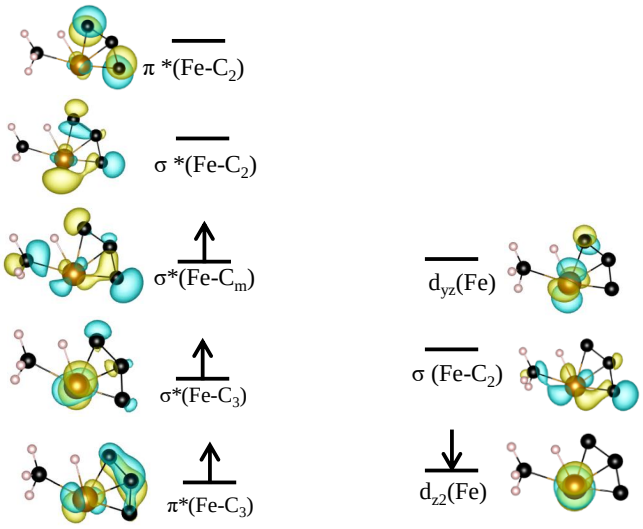


(b) TS1

Figure S6: Kohn-Sham orbital diagram of methane activation process on $FeC_3$ cluster for IS and TS1. The up and down arrows represent the alpha and beta spin electrons. The isosurface value used is 0.07 $a_0^{-3}$.

# 6 The H-transfer in nonet channel of $Fe_3C$

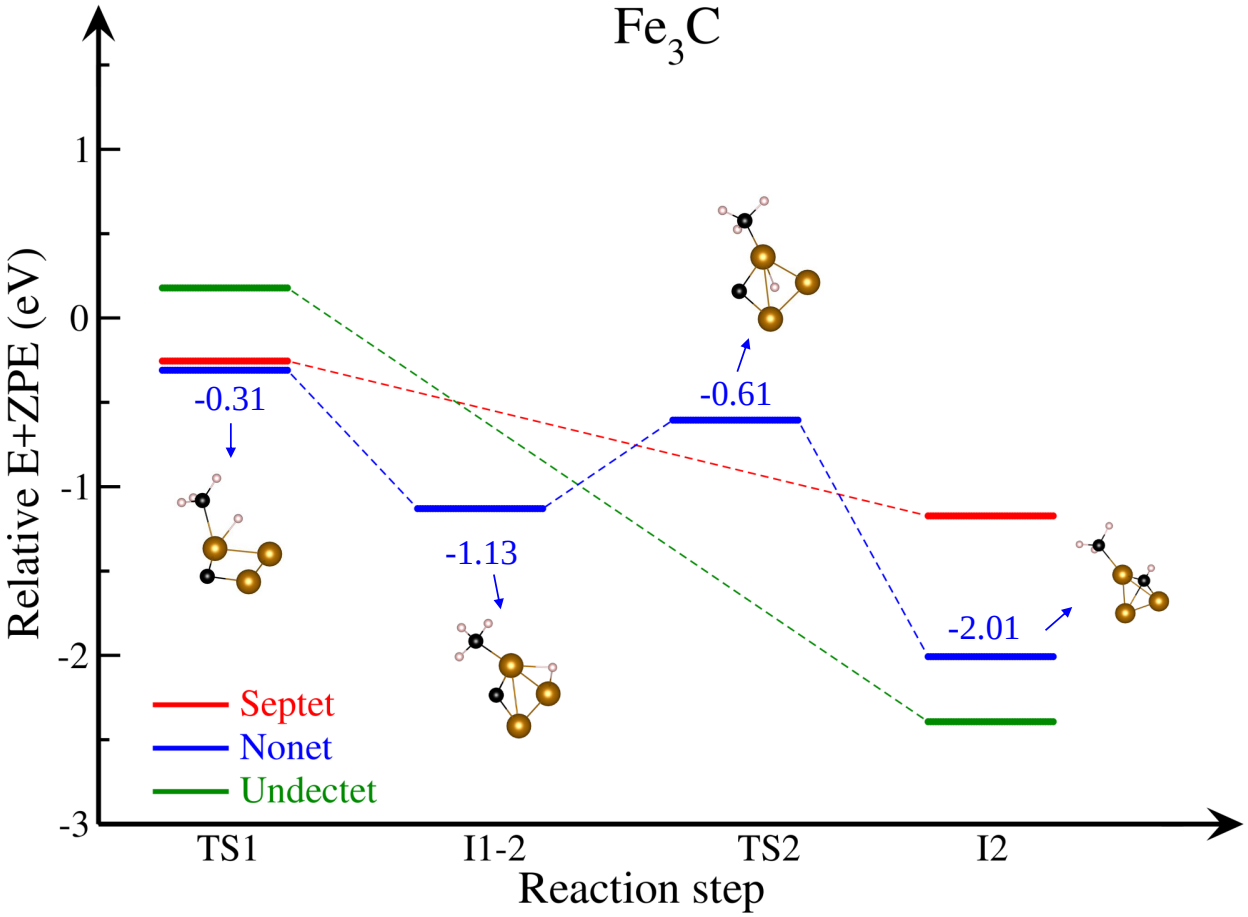


(a) $Fe_3C$

Figure S7: Elementary steps between TS1 and I2 in nonet channel of $Fe_3C$.

# 7 Free energy profile computed with TPSSh/OPBE level

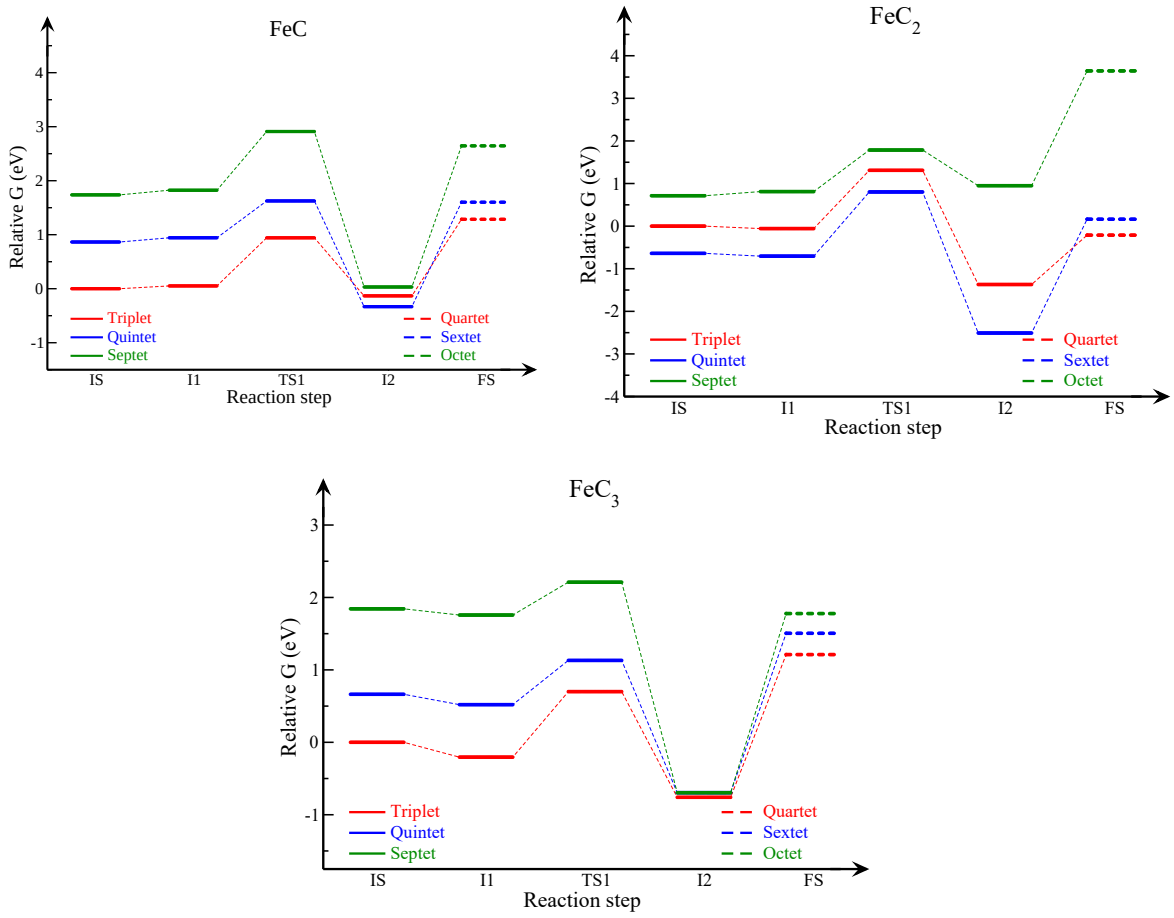


Figure S8: Reaction pathways for methane activation and methyl radical evolution over mononuclear clusters in three lowest energy spin multiplicity states using TPSSh/OPBE level of theory.

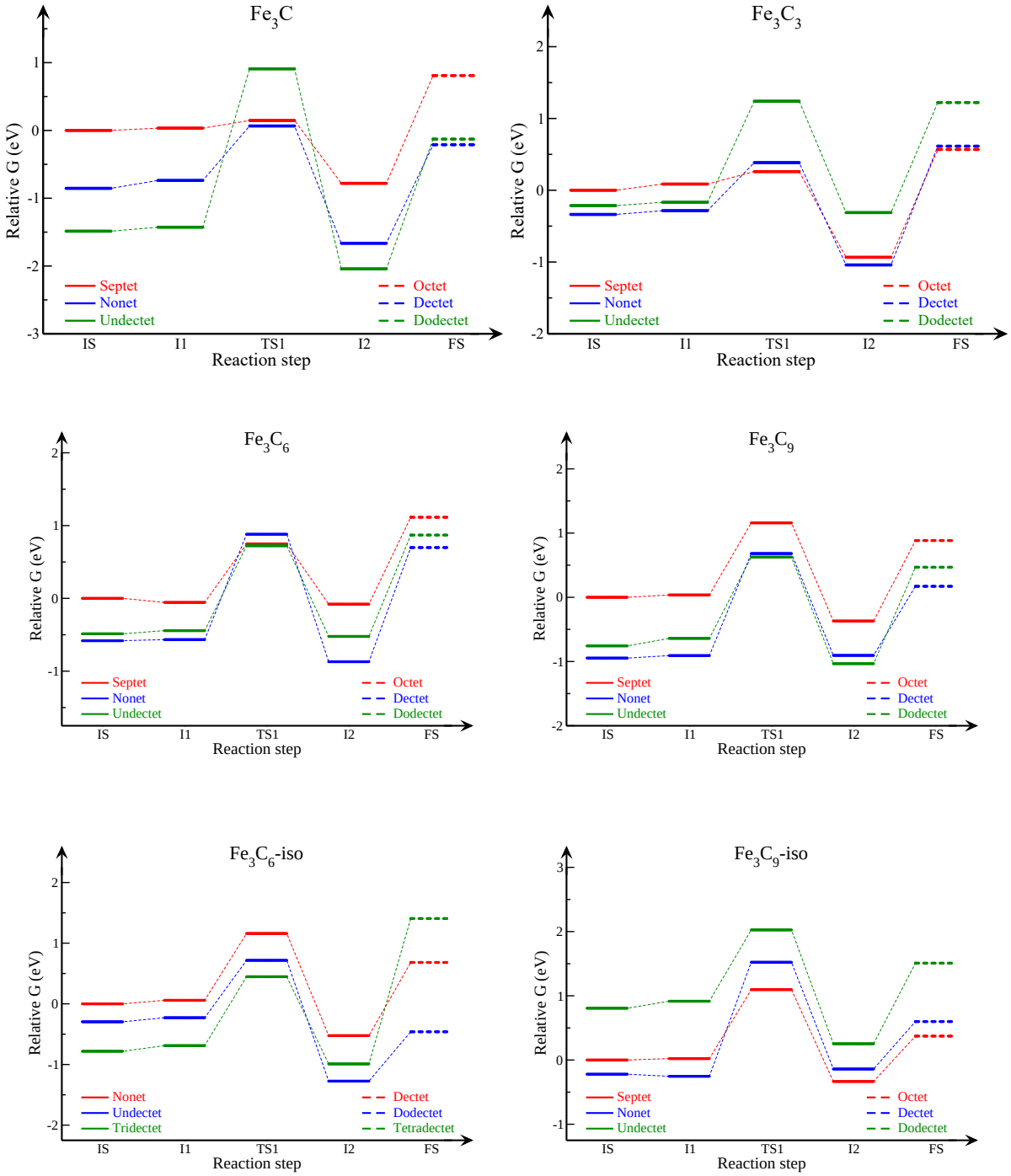


(f) Free energy

Figure S9: Reaction pathways for methane activation and methyl radical evolution over trinuclear clusters in three lowest energy spin multiplicity states using TPSSh/OPBE level of theory.

# 8 Potential energy profile and free energy profile computed with OPBE level

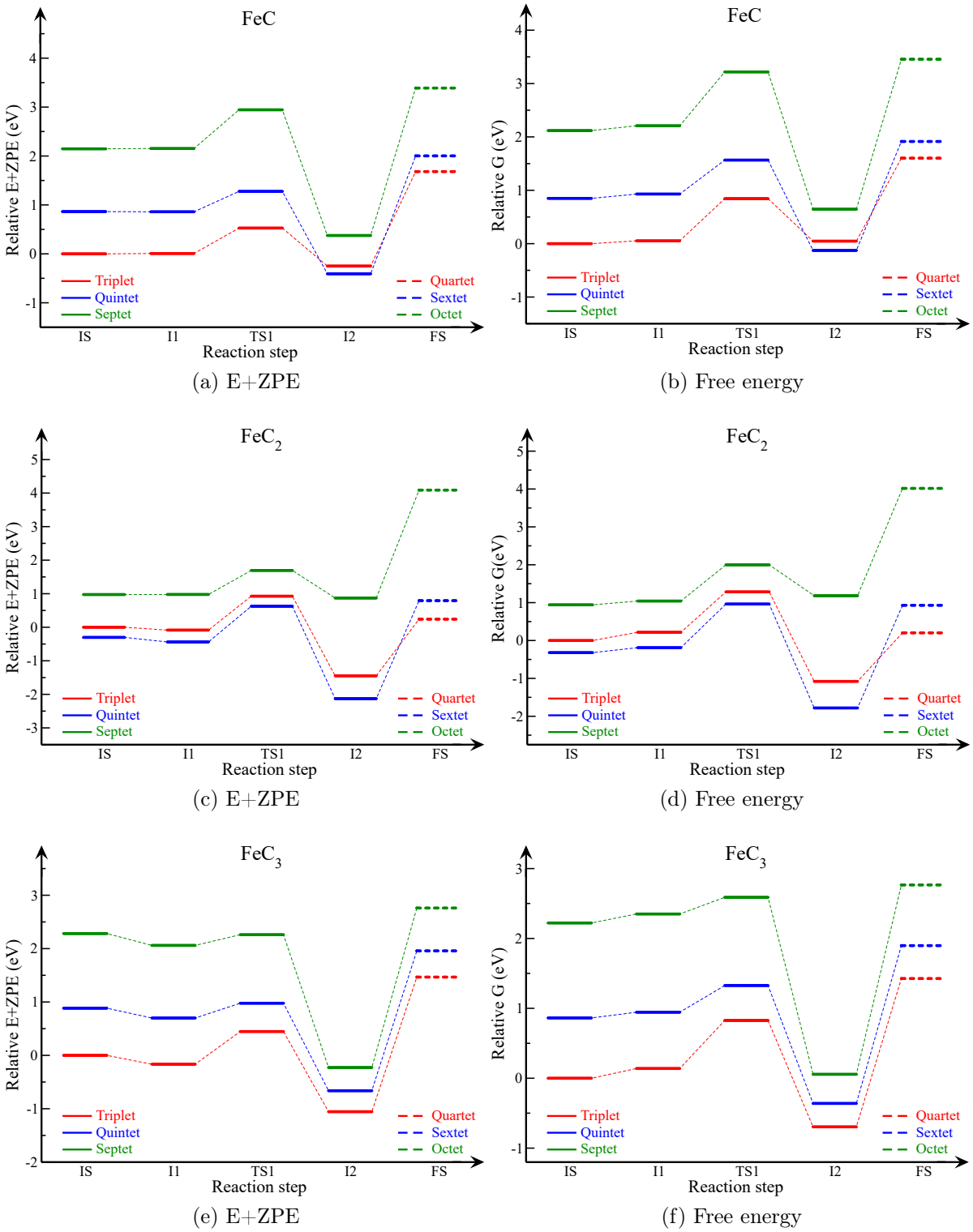


Figure S10: Reaction pathways for methane activation and methyl radical evolution over mononuclear clusters in three lowest energy spin multiplicity states using OPBE/def2TZVP level of theory.

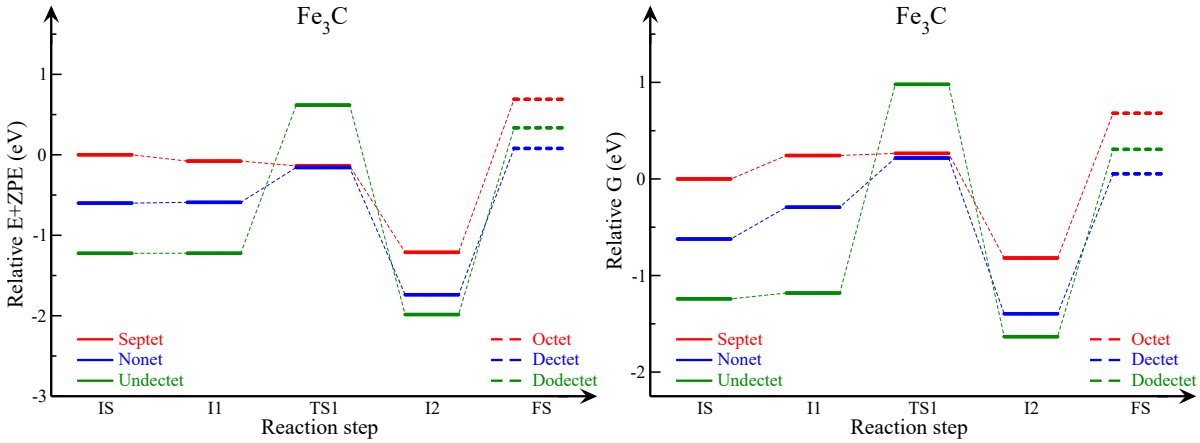


(a) E+ZPE (b) Free energy

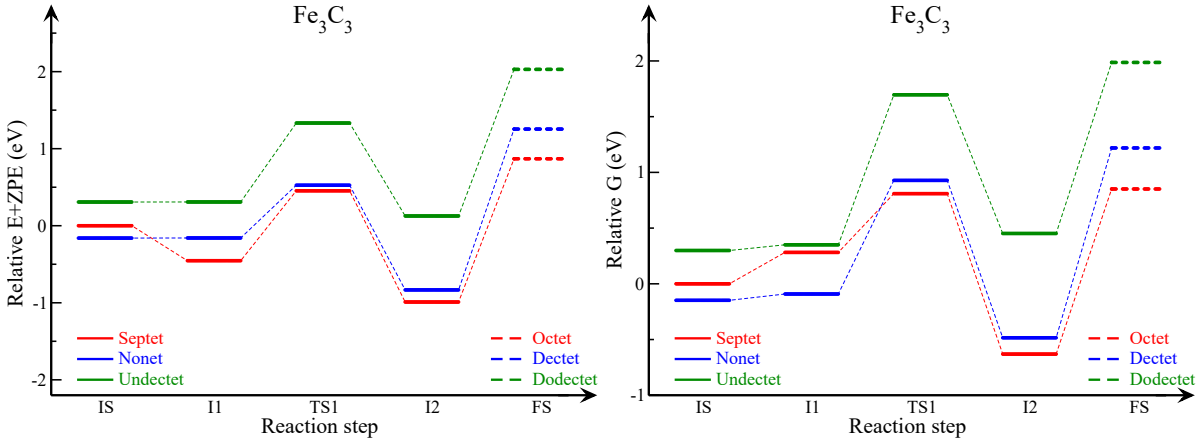


(c) E+ZPE (d) Free energy

Figure S11: Reaction pathways for methane activation and methyl radical evolution over trinuclear clusters - $Fe_3C$ and $Fe_3C_3$ - in three lowest energy spin multiplicity states using OPBE/def2TZVP level of theory.

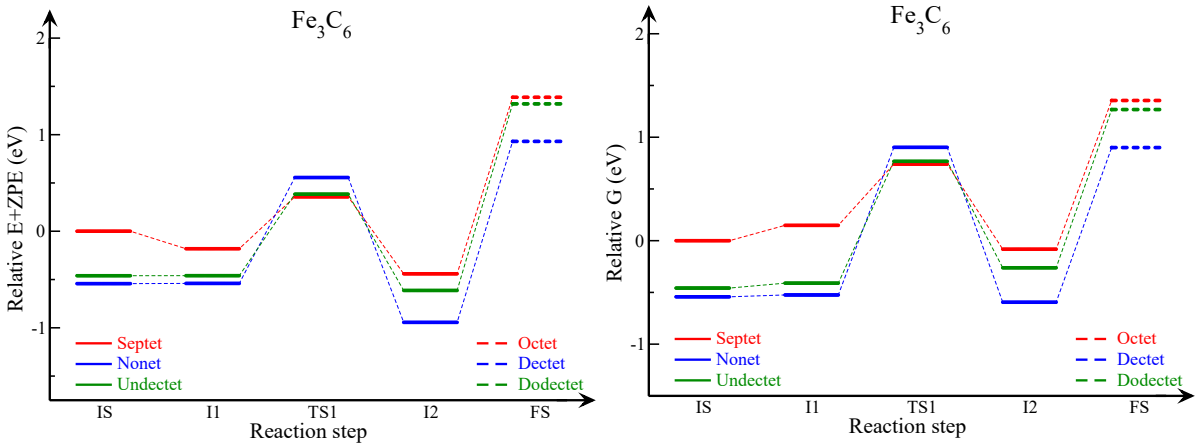


(a) E+ZPE




(b) Free energy

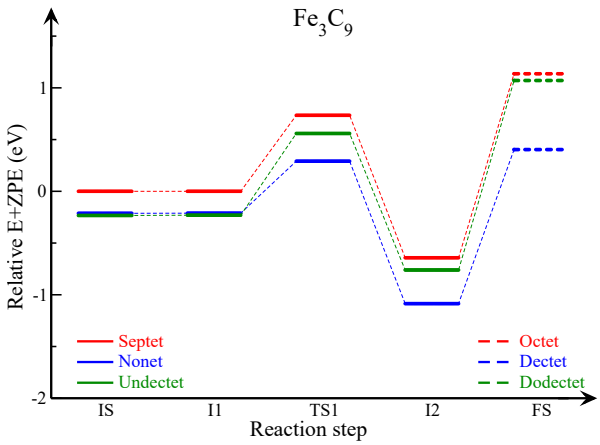


(c) E+ZPE

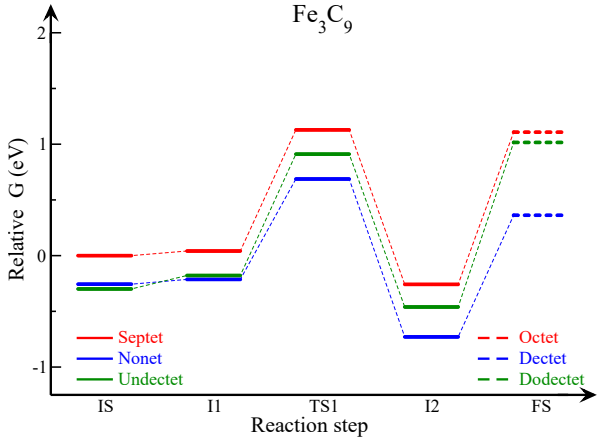


(d) Free energy

Figure S12: Reaction pathways for methane activation and methyl radical evolution over trinuclear clusters - $Fe_3C$ and $Fe_3C_3$ - in three lowest energy spin multiplicity states using OPBE/def2TZVP level of theory.

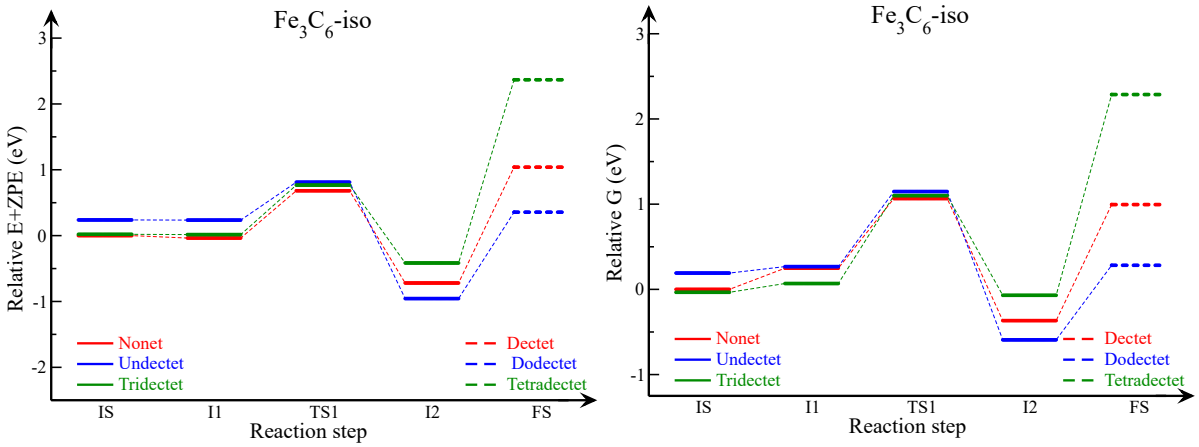


(a) E+ZPE (b) Free energy

(c) E+ZPE (d) Free energy

Figure S13: Reaction pathways for methane activation and methyl radical evolution over high energy isomer $Fe_3C_6$-iso and $Fe_3C_9$-iso triuclear clusters in three lowest energy spin multiplicity states using OPBE/def2TZVP level of theory.

# References


(1) Perdew, J. P.; Burke, K.; Ernzerhof, M. Generalized Gradient Approximation Made Simple. *Phys. Rev. Lett.* **1996**, *77*, 3865–3868.

(2) Becke, A. D. Density-functional exchange-energy approximation with correct asymptotic behavior. *Phys. Rev. A* **1988**, *38*, 3098.

(3) Perdew, J. P. Density-functional approximation for the correlation energy of the inhomogeneous electron gas. *Phys. Rev. B* **1986**, *33*, 8822.

(4) Perdew, J. P.; Wang, Y. Accurate and simple analytic representation of the electron-gas correlation energy. *Phys. Rev. B* **1992**, *45*, 13244.

(5) Zhang, Y.; Wu, A.; Xu, X.; Yan, Y. OPBE: A promising density functional for the calculation of nuclear shielding constants. *Chem. Phys. Lett.* **2006**, *421*, 383–388.

(6) Zhao, Y.; Truhlar, D. G. A new local density functional for main-group thermochemistry, transition metal bonding, thermochemical kinetics, and noncovalent interactions. *J. Chem. Phys.* **2006**, *125*, 194101.

(7) Reiher, M.; Salomon, O.; Hess, B. A. Reparameterization of hybrid functionals based on energy differences of states of different multiplicity. *Theor. Chem. Acc .* **2001**, *107*, 48–55.

(8) Csonka, G. I.; Perdew, J. P.; Ruzsinszky, A. Global hybrid functionals: A look at the engine under the hood. *J. Chem. Theory Comput.* **2010**, *6*, 3688–3703.

(9) Raghavachari, K.; Trucks, G. W. Highly correlated systems. Excitation energies of first row transition metals Sc–Cu. *J. Chem. Phys.* **1989**, *91*, 1062–1065.

(10) Weigend, F.; Ahlrichs, R. Balanced basis sets of split valence, triple zeta valence and quadruple zeta valence quality for H to Rn: Design and assessment of accuracy. *Phys. Chem. Chem. Phys.* **2005**, *7*, 3297–3305.

(11) Schäfer, A.; Huber, C.; Ahlrichs, R. Fully optimized contracted Gaussian basis sets of triple zeta valence quality for atoms Li to Kr. *J. Chem. Phys.* **1994**, *100*, 5829–5835.

(12) Swart, M.; Güell, M.; Luis, J. M.; Sola, M. Spin-state-corrected Gaussian-type orbital basis sets. *J. Phys. Chem. A* **2010**, *114*, 7191–7197.

(13) Schäfer, A.; Horn, H.; Ahlrichs, R. Fully optimized contracted Gaussian basis sets for atoms Li to Kr. *J. Chem. Phys.* **1992**, *97*, 2571–2577.

(14) Limon, P.; Miralrio, A.; Castro, M. Characterization of Magnetic Series of Iron–Carbon Clusters Fe n C0,±1 (n $\leq$ 13). *J. Phys. Chem. C* **2020**, *124*, 9484–9495.

(15) Lide, D. *Handbook of Chemistry and Physics; CRC Press: Boca Raton, U.S.A.*; 2003.

(16) Brugh, D. J.; Morse, M. D. Optical spectroscopy of jet-cooled FeC between 12000 and 18100 $cm^{-1}$. *J. Chem. Phys.* **1997**, *107*, 9772–9782.